ISTITUTO NAZIONALE DI FISICA NUCLEARE

Laboratori Nazionali
di Legnaro

U. Fasoli, G. Galeazzi, I. Scotoni, D. Toniolo and G. Zago :
NEUTRON SCATTERING FROM ^{23}Na, ^{27}Al, ^{28}Si AT 14 MeV.

Istituto Nazionale di Fisica Nucleare
Laboratori Nazionali di Legnaro

U. Fasoli, G. Galeazzi, I. Scotoni, D. Toniolo and G. Zago : NEUTRON SCATTERING FROM ^{23}Na, ^{27}Al, ^{28}Si AT 14 MeV[x]. -

ABSTRACT. -

The scattering of 14 MeV neutrons from ^{23}Na, ^{27}Al and ^{28}Si has been experimentally studied by means of the time-of-flight technique. A 400 keV pulsed ion accelerator has been used as neutron source.

For ^{23}Na the differential cross section of the elastic and inelastic scattering has been measured in the angular interval 20° - 130° and the results are compared with the previsions of the optical model.

For ^{27}Al and ^{28}Si the differential cross section has been measured at 60°.

INTRODUCTION. -

The interaction of neutrons with sodium has been recently investigated by several authors both experimentally and theoretically, owing to the interest of sodium as coolant for fast reactors. Furthermore, since ^{23}Na is considerably deformed, it is of preminent interest to study the interaction of fast neutrons with this nucleide.

The energy range between 1.5 and 4.0 MeV has been previously studied by Towle and Gilboy[1]. Subsequently, measurements have been estended up to the energy of 6.4 MeV in this laboratory[2]. Very recently the same authors[2] performed experiments of elastic and inelastic scattering of neutrons at the two energies of 8.0 and 10 MeV on ^{23}Na, ^{27}Al and ^{28}Si[3].

It has been considered worthwhile measuring the scattering differential cross section at the neutron energy of 14 MeV on the same

_____

(x) - Work performed under CNEN-Università di Padova Contract at the Laboratori Nazionali di Legnaro (INFN).

2.

nuclei and particularly on ^{23}Na for which no results are up to now avai
lable.

The experiment has been performed using the facilities of a
new 400 keV pulsed ion accelerator recently installed at the Legnaro
Laboratory. In this report we describe the experiment and give some
details on the accelerator itself. The optical model analysis of the data,
including also those taken for the other energies and for the other two
nuclei, is in progress and will be published elsewhere.

THE ACCELERATOR AND THE PULSING SYSTEM. -

The 14 MeV neutrons used in this experiment have been produ
ced by the (d, t) reaction in a thick tritium-zirconium target. The radio-
frequency ion source of the accelerator supplies a continuous deuteron
ion beam of about 0.5 mA. The ion beam accelerated up to 20 keV is
focused on a metal screen having a 2 mm circular hole by means of a
triplet of magnetic quadrupoles[4]. With this optics the transmission
through the hole of the ions having a charge to mass ratio different from
the singly charged deuteron ions is negligible. The pulsing operation is
achieved in the manner previously divised at Oak Ridge[5]. The beam
spot on the screen is moved along an ellipsis by means of two crossed
R.F. electrostatic fields. The ion bursts outcoming from the hole at
the frequency of 1 or 3×10^6 s^{-1} are about 10 ns long. They are bunched
up to about 1.5 ns on the tritium target by means of an axial R.F. com
pressor located between the hole and the accelerating tube.

The beam is accelerated by means of a high voltage generator,
manufactured by SAMES, which can provide a current of 3 mA at a ma-
ximum voltage of 400 kV. The high voltage is stabilized to 1% and can
be varied continously. The source and the accelerator tube are contained
in an iron tank filled with carbonitrogen at 15 atm pressure. The accele
rated beam is bent on the horizontal plane by means of a deflecting mag
net. The beam can be sent to any direction by rotating the magnet. A
capacitive pick up located before the target gives signals synchronous
to the beam pulses. The pick up pulses, properly delayed, act as "stop"
signals to measure the neutron time-of-flight.

EXPERIMENTAL METHOD. -

The experimental arrangement is schematically given in Fig. 1.
The deuteron beam hits the tritium-zirconium target T flying normal to
the figure plane. The neutrons emitted at 90$^{\mathrm{o}}$ are scattered by the scat
terer S towards the neutron detector D through a hole in the concrete
wall 2 m thick. An iron shadow bar improves the screening between the
source and the detector. The neutron flight base is 4 m. The detector M
acts as monitor of the neutron yield from the target. The three scatterers
used were all cylindrical with the following characteristics:

- sodium : contained in a very light aluminum can, with diameter 3.0 cm and 6.0 cm height ; mass 49 g;
- aluminium : diameter 3.0 cm, height 10.0 cm, mass 188 g;
- silicon : diameter 2.9 cm, height 11.0 cm, mass 170 g.
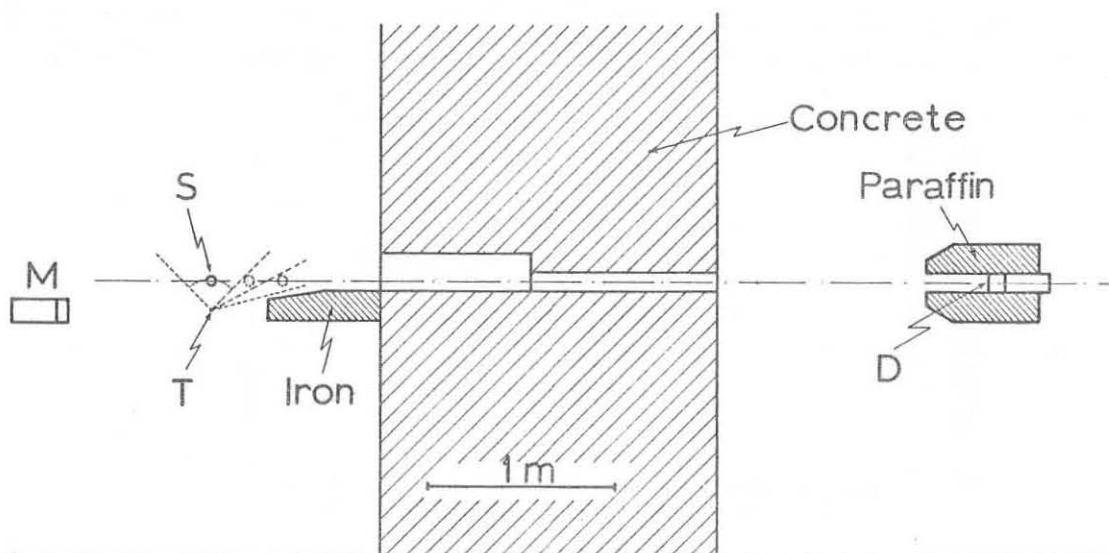
FIG. 1 - Experimental lay-out. T, tritium target (the deuteron beam flies normal to the figure plane). S, scatterer. D, scattered neutron detector. M, neutron monitor.

The axes of the scatterers were parallel to the deuteron beam. The detector D was fixed; the scattering angle was varied by rotating the scatterer around the deuteron beam axis. The target-to-scatterer distance was 32 cm for scattering angles between 20° and 32.5^{o}, 20 cm and 15 cm respectively for the others two angular intervals 35°-55° and 60°-130°. The measurements at different angles were normalized by taking into account the different geometries.

DETECTORS AND ELECTRONICS. -

The neutron detection system was formed by two time-of-flight scintillation counters, the first acting as monitor of the neutrons produced by the target and the second as detector of the scattered neutrons. Both scintillators were liquid NE213, the monitor was 5 cm in diameter and 2.5 cm thick and the main counter 10 cm in diameter and 5 cm thick. The two scintillators were followed by a 56 AVP and a XP 1040 photomultiplier respectively. The time-of-flight electronics was of conventional type based on the time-to-pulse height conversion. The "stop" pulse was supplied by the pick-up located before the target, as described before. The main counter electronic chain incorporated a gamma ray discrimination circuit. A block diagram of the electronics is given in ref. (6).

4.

NEUTRON DETECTION EFFICIENCY. -

The neutron detection efficiency as a function of energy of the main detector has been determined by scattering from a small polietylene sample with a mass of 12 g; the carbon contribution was subtracted by scattering from a graphite sample. The relative efficiency curve is given in Fig. 2. The fall of the efficiency below ~ 4 MeV is due to an electronic bias on the amplitude of the pulses from the photomultiplier.
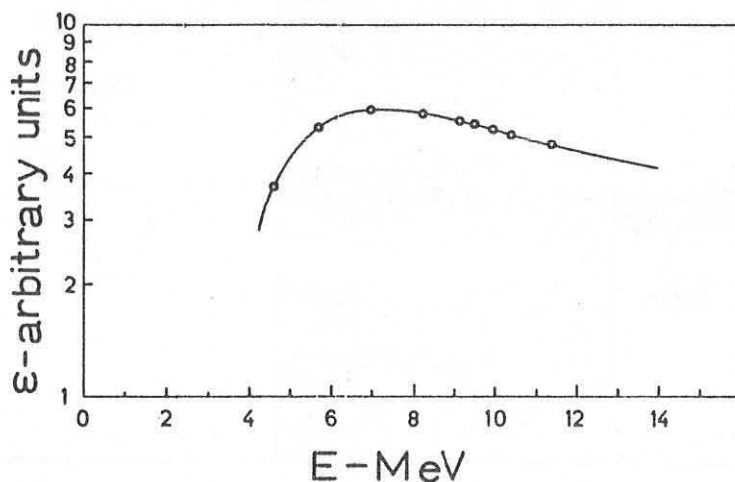
FIG. 2 - Relative efficiency of the neutron detector as a function of the neutron energy.

Its position has been chosen on the basis of a compromise between the signal due to the scattered neutrons and the noise due to the background. The bias was controlled by observing the amplitude spectrum of the pulses generated by a ^{60}Co source.

TIME AND ENERGY RESOLUTION. -

The form of the deuteron pulse observed after the deflecting magnet by means of a co-axial target and a sampling oscilloscope is represented in Fig. 3. The oscillations after the pulse are due to reflection on the cables.
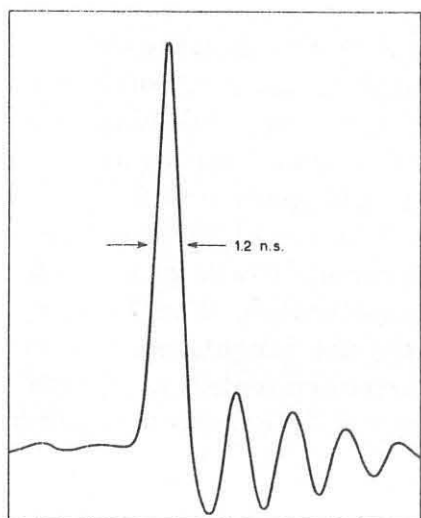
The overall time resolution of the scattering neutrons, as it appears from Fig. 8, is around 3 ns at half height of the elastic peak. The most important contri-

FIG. 3 - The form of deuteron beam pulse observed with a Faraday co-axial cup and a sampling oscilloscope. The oscillations after the pulse are due to reflection on the cables.

butions to the pulse width are : the width of the deuteron bursts (1.5 ns), the geometry of the tritium target which was 45 degrees inclined with respect to the deuteron beam (1 ns), the thickness of the detector (1.2 ns), the time resolution of the electronics (0.8 ns). The energy resolution is given by the relation

$$\Delta E = 27.8 \, \frac{\Delta t}{D} \, E^{3/2} \qquad (\Delta E \text{ keV}, \quad E \text{ MeV}, \quad \Delta t \text{ ns}, \quad D \text{ m}).$$

With the flight base of 4 m adopted in the present experiment the neutron energy resolution is of 1.1 MeV for 14 MeV neutrons and of 0.22 MeV for 5 MeV neutrons.

RESULTS. -

^{23}Na

The angular distribution of the elastic and inelastic scattering from ^{23}Na has been measured by taking time-of-flight spectra at several angles between 20° and 130°.

A typical spectrum taken at 90° is shown in Fig. 4. The first
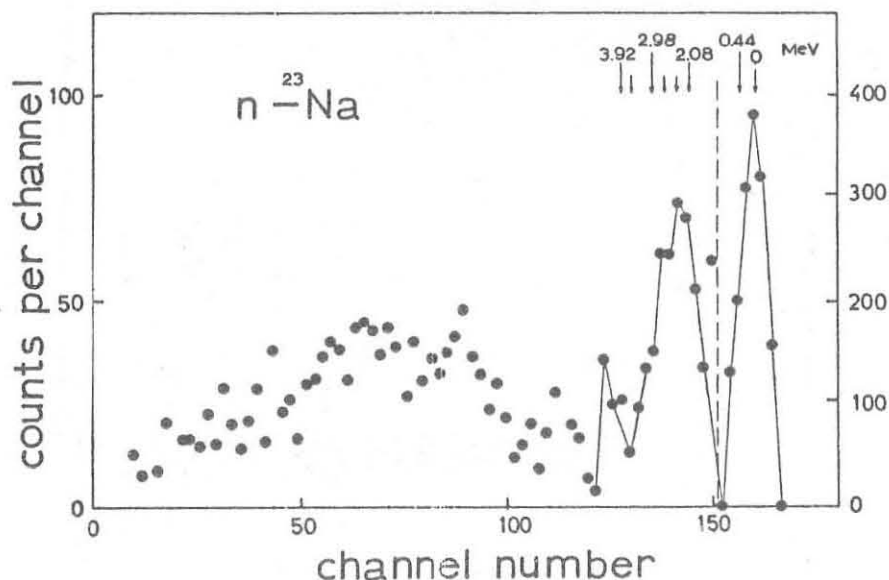
FIG. 4 - Time-of-flight spectrum of the neutrons scattered at 90° by ^{23}Na. Time-of-flight base 4 m; time scale 0.8 ns/channel. The arrows correspond to the expected position of the inelastic neutrons peaks from the indicated ^{23}Na levels.

^{23}Na level of 0.44 MeV is not resolved from the ground state level. The groups of levels having Q between 2 and 3 MeV give rise to a large peak where the levels with lower Q-values are predominant; the levels having Q larger than about 4 MeV give rise to a continuous spectrum with a form which is typical of an evaporation process.

6.

The calculation of differential cross section has been performed by comparison with the n-p cross section with the method explained in a precedent work[2].

The results are given in Fig. 5 and Table I. The inelastic differential cross section relative to the groups of levels between 2 and 3 MeV has been given only at four angles where the measurements were repeated to decrease the statistical error.
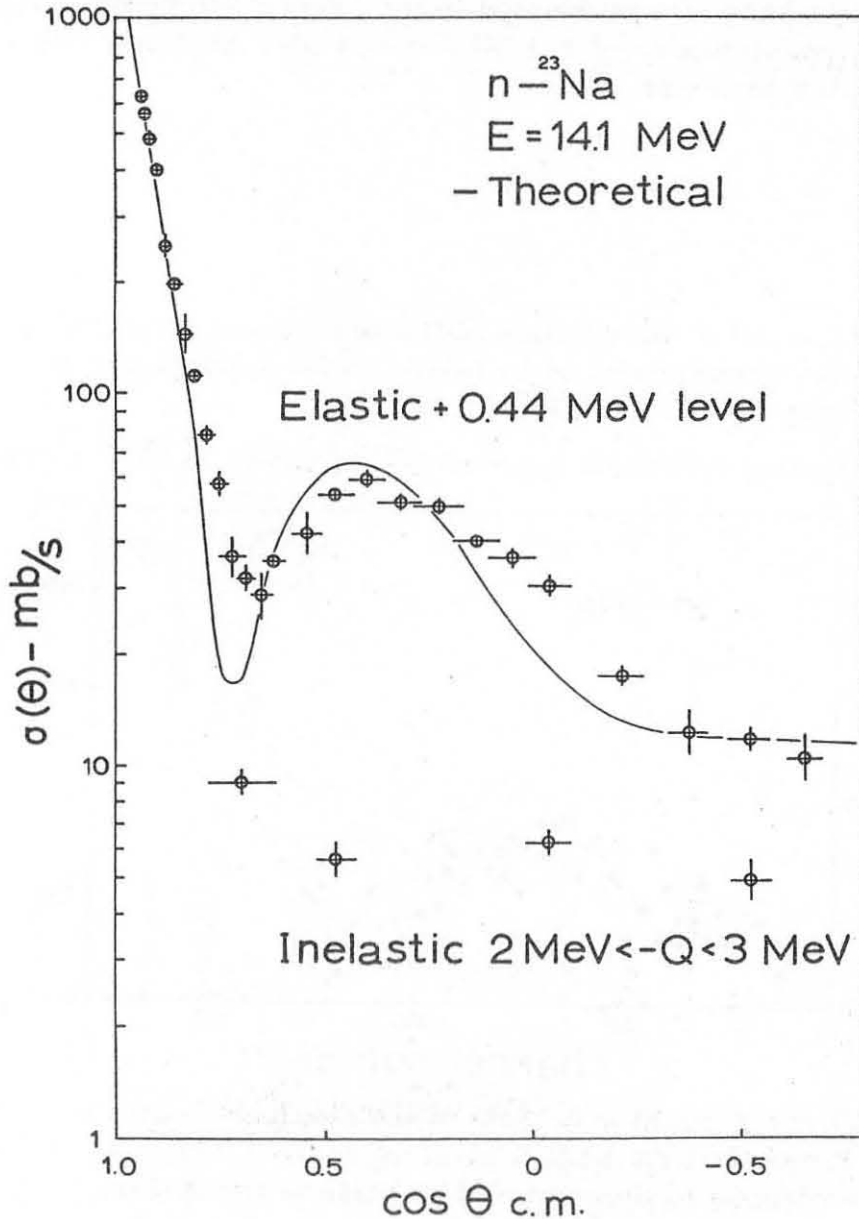
FIG. 5 - Differential cross section of the scattering of 14.1 MeV neutrons from ^{23}Na. The vertical bars are the statistical errors. The horizontal bars represent the angular resolution. The continuous curve is theoretical (see text). The data are not corrected for the multiple scattering.

TABLE I

Differential cross section of 14 MeV neutron scattering from the ground state plus 0.44 MeV levels of ^{23}Na. The indicated cross section values are not corrected for the attenuation in the scatterer and for the multiple scattering. The errors are statistical.

ψ_{lab}	$\cos\theta_{c.m.}$	$\sigma(\theta)$ - mb/s	$\pm\Delta\%$	ψ_{lab}	$\cos\theta_{c.m.}$	$\sigma(\theta)$ - mb/s	$\pm\Delta\%$
20°	0.9385	630.1	3.5	50°	0.6163	35.5	4.6
21°	0.9309	563.7	2.5	55°	0.5410	42.2	12.0
22.5°	0.9194	486.0	4.2	60°	0.4717	54.3	2.5
25°	0.9002	398.0	2.8	65°	0.3899	58.8	4.7
27.5°	0.8768	251.0	7.7	70°	0.3056	51.0	3.5
30°	0.8535	197.4	3.7	75°	0.2193	50.0	4.6
32.5°	0.8318	144.6	12.0	80°	0.1319	39.9	3.2
35°	0.8102	112.4	3.8	85°	0.0441	36.1	6.0
37.5°	0.7809	77.6	6.6	90°	-0.0435	30.6	3.9
40°	0.7516	58.5	8.3	100°	-0.2151	17.2	5.8
42.5°	0.7192	36.6	13.0	110°	-0.3781	12.2	14.0
45°	0.6867	31.9	7.9	120°	-0.5282	11.8	6.4
47.5°	0.6515	28.6	16.0	130°	-0.6617	10.5	15.0

The reported data are not corrected for the multiple scattering in the scatterer, but from previous measurements[2] they turn out to be not larger, in the average, than about 10%. The correction will be done together with the optical model analysis.

^{27}Al

The time-of-flight spectrum of the neutrons scattered by ^{27}Al at 60° is shown in Fig. 6, together with the background spectrum. The characteristic peak in the latter is believed to be due to the scattering from the air surrounding the scatterer.

The "elastic" peak contains also the contribution of the doublet of levels having Q of 0.842 and 1.013 MeV. The energy spectrum of the inelastic neutrons represented in Fig. 7 as a plot of log $\sigma(E)/E$ versus E is well fitted with a straight line, as predicted by the statistical model. The corresponding nuclear temperature, calculated from the slope of the straight line of Fig. 7 is 2.5 ± 0.1 MeV. This value is quite different from the corresponding values of 0.7 MeV measured by Graves[7] and 1.06 of O'Neill[8], relative to emitted neutrons energy intervals between 1 and 5 MeV and incident neutron energy of 14 MeV. Thomson[9]

8.

found T = 0.96 ± 0.15 MeV for the ^{27}Al for an incident neutron energy of 7.0 MeV.
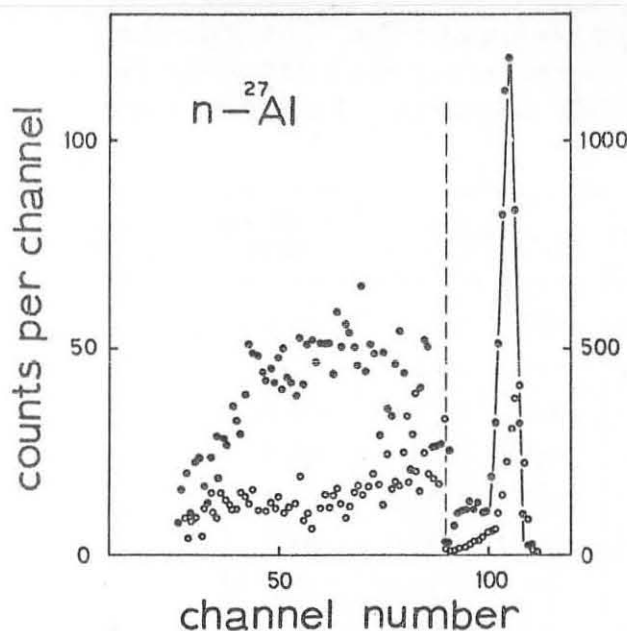
FIG. 6 - Time-of-flight spectrum of neutrons scattered at 60° from ^{27}Al. Time-of-flight base 4 m, time scale 0.8 ns per channel. o o o Background.
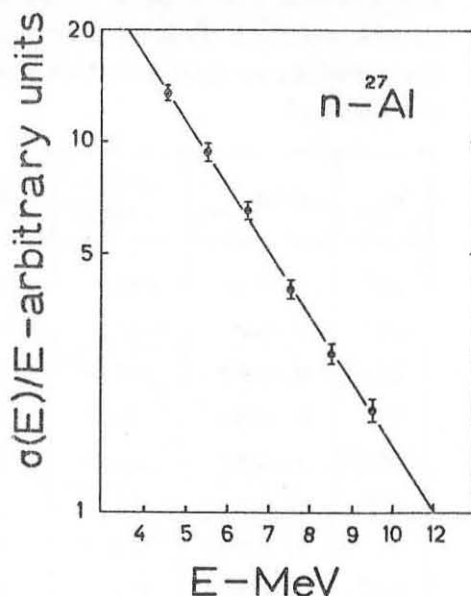
FIG. 7 - Energy spectrum of the neutrons scattered by ^{27}Al as a plot of $\sigma(E)/E$ versus the scattered neutron energy E.

The dependence of the nuclear temperature from the incident neutron energy and from the emitted neutron energy has been observed also by other authors[10] and may be explained by the different reaction mechanism present at different energies[11].

^{28}Si

The time-of-flight spectrum of the neutrons scattered by ^{28}Si at 60° is shown in Fig. 8. The first inelastic 1.77 MeV (2$^+$) level is almost completely resolved from the ground state level.

The differential cross sections relative to single levels or group of levels are reported in Table II together with the recent results of refs. (12, 13). Taking into account the errors, the agreement may be considered to be good.

The comparison of the spectrum of Fig. 8 with the similar spectrum obtained by the authors of ref. (12), Fig. 2 indicates that in the present work with an energy resolution about equal, the signal to background ratio is an order of magnitude better. We believe that this is due to the presence of the gamma ray discrimination circuit and to our heavier screening.

Figure 8 shows also which is the energy resolution in scattering experiments. The risolution may be improved by using a neutron
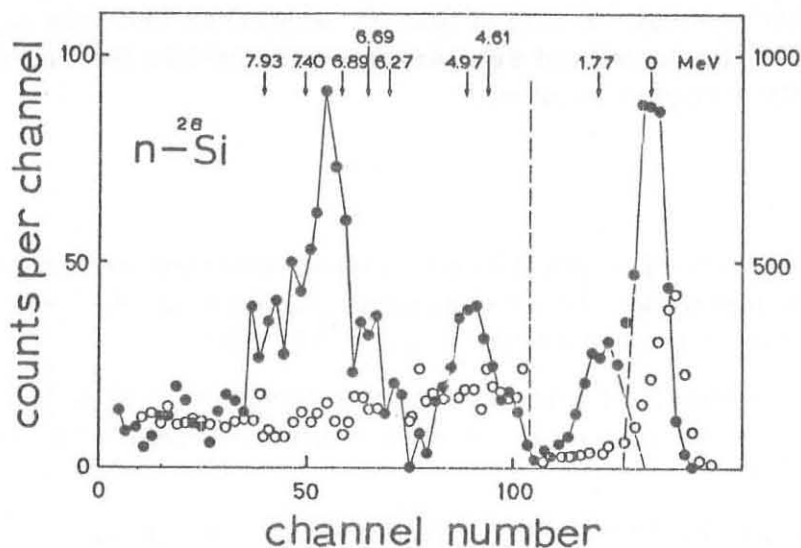
FIG. 8 - Time-of-flight spectrum of the neutrons scat tered at 60° from ^{28}Si. Time-of-flight base 4 m; time scale 0.8 ns per channel. The arrows correspond to the expected position of the inelastic neutron peak from the indicated ^{28}Si levels. ooooo Background.

source of higher intensity, for example a duoplasmatron source, which would allow to increase the neutron flight base. An increase of a factor 10 in the average pulsed current (of about 10 μA in the present experiment), which is technically possible, would increase the energy resolu tion of a factor 3 remaining unchanged the measuring time (30-60 minu tes per spectrum).

TABLE II

Elastic and inelastic differential cross section of 14 MeV neu-tron scattering from ^{28}Si, at 60°.

	-Q, MeV	0	1.77	4.61+4.97	6.27	6.69	6.89+7.40	7.93
(a)	σ (mb/s)	45*	11.6±0.3	2.3±0.1	0.3±0.1	0.9±0.1	3.3±0.2	1.3±0.1
(b)	σ (mb/s)	45	10±1	2.0±0.5	0.6±0.2			
(c)	σ (mb/s)	45	10±2	3±1				

(a) - Present work, (*) normalized to the values of refs. (12) and (13). The indicated errors are statistical.
(b) - Ref. (12).
(c) - Ref. (13).

In the elastic scattering time-of-flight region the larger back-ground source is due to the scattering from the air surrounding the neu tron source (Figs. 6, 8). The background to signal ratio is negligible in the forward scattering, but it is high in the backward scattering, where

the cross sections are very small. The situation would be improved by evacuating the air around the target and the scatterer but only a predo-minant interest in the backward scattering would justify the adoption of this mechanically complex solution.

CONCLUSION. -

The facilities of a new 400 keV ion accelerator at the Legnaro Laboratory, employed as a 14 MeV neutron pulsed source, have been used in a scattering experiment on ^{23}Na, ^{27}Al, ^{28}Si.

The main result of this work is the differential elastic and ine-lastic scattering cross section of 14 MeV neutrons from ^{23}Na, not yet measured up to now.

A first comparison with the theoretical previsions is shown in Fig. 5. The continuous curve has been obtained by adding the contribu-tion of the inelastic 0. 44 MeV level, taken as equal to the one measured by Crawley and Garvey[15] in a proton-^{23}Na scattering experiment at 17. 5 MeV, to the elastic cross section calculated by Agee and Rosen[14] by a local potential with average parameters. The agreement with the experimental results is satisfactory only for the very small and large angles.

An analysis of our results from 1. 5 to 14 MeV in terms of the optical model which takes into account also the ^{23}Na deformation is in progress, following the procedure used in ref. (2).

REFERENCES. -

(1) - J. H. Towle and W. B. Gilboy, Nuclear Phys. 32, 610 (1962).

(2) - U. Fasoli, D. Toniolo, G. Zago and V. Benzi, Nuclear Phys. A125, 227 (1969).

(3) - U. Fasoli, D. Toniolo and G. Zago, unpublished.

(4) - I. Scotoni and G. Galeazzi, University of Padua, unpublished.

(5) - G. D. Moak, W. M. Good, R. F. King, J. W. Johnson, H. E. Banta, J. Judish and W. H. du Preez, Rev. Sci. Instr. 35, 672 (1964).

(6) - V. Benzi, U. Fasoli, D. Toniolo and G. Zago, CNEN Report, Doc. CEC(68)7 (1968).

(7) - E. R. Graves and L. Rosen, Phys. Rev. 89, 343 (1953).

(8) - G. K. O'Neill, Phys. Rev. 95, 1235 (1954).

(9) - D. B. Thomson, Phys. Rev. 129, 1649 (1963).

(10) - R. R. Borchers, R. M. Wood and C. H. Holbrow, Nuclear Phys. 88, 689 (1966); V. B. Anufrienko et al., Antwerp Neutron Conference, 1965 (North Holland, 1966), Contribution n. 197.

(11) - R. Batchelor, Proc. of the Neutron Conf., Antwerp, 1965 (North Holland, 1966).

(12) - J. Höhn, H. Pose and D. Seeliger, Nuclear Phys. A134, 289 (1969).

(13) - P. H. Stelson, R. L. Robinson, H. J. Kim, J. Rapaport and G. R. Satchler, Nuclear Phys. 68, 97 (1965).

(14) - F. P. Agee and L. Rosen, Report LA-3538-MS (1966).

(15) - G. M. Crawley and G. T. Garvey, Phys. Rev. 167, 1070 (1968).